Article

Effectiveness of the autonomous braking and evasive steering system OPREVU-AES in real world vehicle-to-pedestrian collisions

Ángel Losada[1,*], Francisco Javier Páez[1] , Francisco Luque[2] and Luca Piovano[2]

[1] Department of accidentology, University Institute for Automobile Research Francisco Aparicio Izquierdo (INSIA-UPM) Universidad Politécnica de Madrid. 28031 Madrid, Spain
[2] Center for Energy Efficiency, Virtual Reality, Optical Engineering and Biometry (CEDINT-UPM) Universidad Politécnica de Madrid. 28223 Pozuelo de Alarcón, Spain
* Correspondence: angel.losada.arias@upm.com; Tel.: +34-616-909-632

Abstract: Among the possible improvements of Autonomous Emergency Braking (AEB) systems, reducing the intensity of the automatic braking process by studying the kinematics and general behavior of the pedestrian while crossing is crucial to determine the progressiveness of the braking, or replacing part of the braking process by an evasive maneuver when a collision is imminent. This paper proposes the integration of an autonomous avoidance system (Automatic Emergency Steering, AES) that acts directly on the steering system to generate an evasive maneuver and avoid a possible pedestrian collision (OPREVU-AES system), as well as the assessment of its effectiveness compared to a commercial AEB system. OPREVU and VULNEUREA are research projects in which INSIA and CEDINT have cooperated to improve driving assistance systems and the safety of pedestrians and cyclists through Virtual Reality (VR) techniques. The analysis of the kinematic and dynamic response of the OPREVU-AES system is conducted in CarSim© software. The effectiveness evaluation procedure is based on the reconstruction of a sample of road vehicle-to-pedestrian crashes (INSIA-UPM database), using the PCCrash® software, and taking as an indicator the probability of head injury severity (ISP). The results show that the AEB system would have prevented part of the collisions, especially after the incorporation of the OPREVU-AES system. In most of the cases where avoidance is not possible, a significant reduction of the ISP is achieved.

Keywords: pedestrian safety, Autonomous Emergency Braking AEB, Automatic Emergency Steering AES, collision reconstruction, probability of head injury severity ISP

1. Introduction

Nowadays, with the aim of increasing road safety and ensuring an effective response by the vehicle when a hazardous situation occurs on the road, Autonomous Emergency Braking (AEB) systems anticipate the driver's response in the event of a potential collision with vehicles and pedestrians or, if a collision occurs, reduce the severity of the damage as much as possible. These systems consist of a fusion sensor, which combines the performance of a camera and a LIDAR (Laser Imaging Detection and Ranging) device.

These systems are the subject of ongoing research aimed at improving both pedestrian behavior identification algorithms and safe avoidance maneuvers [1-2]. Some authors [3] point out possible areas of optimization of AEB systems. Among the possible solutions, it is proposed to regulate the autonomous braking response by acting on the deceleration curve and on the maximum steady-state pressure value, modifying its value as a function of the pedestrian's transverse speed.

The characterization of pedestrian behavior has been studied from the point of view of predicting the pedestrian's trajectory and reaction type [4], using Kalman filters for

 doi:10.20944/preprints202211.0476.v1

image analysis, while other authors [5] focus on the development of Markov decision process (MDP) models for the enhancement of emergency braking systems and autonomous vehicles. In other studies, such as [6], a detection method for walking pedestrians by using a HOG feature to recognize leg crossing is proposed for accident avoidance.

In cases where traffic speeds are high (close to the maximum speed allowed in urban areas in the European Union, 50 km/h), the braking distance may not be sufficient, so new collision avoidance maneuvers are contemplated for the development of Advanced Driver Assistance Systems (ADAS) embedded in new generation vehicles. In particular, the Automatic Emergency Steering system (AES) is placed within the Euro NCAP 2025 roadmap for primary safety [7] and expects further implementation in the fleet from 2022 onwards.

For this reason, a breakthrough system is proposed that is able to integrate a predictive collision model for pedestrians, capable of regulating the braking response at low speeds (below 40 km/h) and generating an automatic evasive maneuver for high speeds (up to 70 km/h) in conditions of maximum safety for other road users and guaranteeing the stability of the vehicle during the whole process, when the necessary distance to execute a braking at maximum pressure is not enough to avoid the accident.

2. State of the art

The integration of an autonomous avoidance system in conjunction with an Autonomous Emergency Braking system has been studied for the avoidance of near-miss conflicts between two vehicles. The combination of both ADAS systems has been tested in [8] in both simulations and real tests, integrating a predictive trajectory system, an autonomous electro-hydraulic braking system and an emergency avoidance system with active front steering.

The execution of evasive maneuvers at high speeds requires sufficient space and the calculation of an intervention point in the decision-making algorithm of the system, which implies a constant calculation of times and distances, such as [9], where trajectory planning involves the integration of a steering feedforward and feedback controller, considering velocities, distances, given maximum acceleration and available space to act. In this paper, trajectory planning is proposed for the control of evasive maneuvers, with the objective of guaranteeing in advance the maneuverability and stability of the vehicle. This approach is similar to that already used in research such as [10], where the design of optimal passing maneuvers involves parameterizing geometric constants (such as lateral clearance distances), dynamic constants (such as longitudinal jerk), and maneuver-end conditions.

Nevertheless, the focus of this survey is on avoiding pedestrian accidents. In [11], the design of the avoidance system revolves around mapping a trajectory with a fuzzy-like control over the steering wheel. Furthermore, the combination of the AEB system with the evasive steering system has been studied in [12], where the decision making of which system is more appropriate at speeds below 50 km/h, in different scenarios with potential hit-and-run situations, has been tested.

In this connection, in order to have a broader and more realistic understanding of pedestrian crossing behavior, the use of Virtual Reality techniques has been carried out for this proposal. Recent articles, such as [13-14], have investigated the applicability of Virtual Reality technology through the use of HMD to study the safety and risk perception (gap choices, perceptual errors, reaction times) of pedestrians when crossing in different virtual environments and with different roads. Additionally, [15] concluded that the deployment of VR controlled environments is valid for studying pedestrian behavior, since the walking speeds of the users are congruent with the average speed of pedestrians crossing in the real world, and the sense of immersion and usability denote the practicality of this methodology.

Through the study of pedestrian-vehicle interaction, some authors, such as [16], have been able to estimate critical zones by calculating the possibility of collision as a function

 doi:10.20944/preprints202211.0476.v1

of the relative lateral and longitudinal distance between car and user. The study of the pedestrian's whole-body kinematics when reacting in such potential hit-and-run situations allows to characterize users behavior, generating avoidance patterns in terms of speed and acceleration for the cases of backward and forward motion.

For the implementation of such improvements, the effectiveness of the new systems in terms of reducing injuries to vulnerable exposed road users [17] should be evaluated prior to their release to the market. The effectiveness measurement indicator used is the Injury Severity Probability (ISP, [18-19]), which estimates the probability of injury to the pedestrian's head as a function of the hit speed and the impact area of the head on the frontal area of the vehicle (hood or windshield).

This paper proposes the formulation of a combined braking and autonomous avoidance system OPREVU-AES, whose operation takes into account the relative distance and speed information obtained by the fusion sensor, as well as the probability of collision as a function of parameters that define the pedestrian's behavior, the pedestrian's level of attention and the visibility conditions of the road. The avoidance trajectories have been predefined for speeds above 40 km/h, controlling the entire overtaking and lane re-entry process by points, thus guaranteeing the lateral stability of the vehicle through the action of the Electronic Stability Control (ESC). Besides, the decision algorithm of this joint system completes its operation by considering the information obtained from the lane line detector and the blind spot detector.

Likewise, this research discusses the results of the evaluation of the effectiveness of the new OPREVU-AES autonomous pedestrian hit-and-run braking and avoidance system, in comparison with a commercial AEB systems. Furthermore, to evaluate whether this type of system would be effective in avoiding collisions in real situations, and whether its implementation would be worthwhile for new generation vehicles, a comparative study of the probability of pedestrian injury is carried out for three scenarios: a vehicle without an ADAS system, a vehicle with an AEB system, and a vehicle with an AEB and AES system for a range of high traffic speeds.

3. Materials and Methods

3.1. Methodology

The methodological scheme (Figure 1) presented in this section has been developed within the Project OPREVU (Grant RTI2018-096617-B-100 funded by MCI/AEI/10.13039/501100011033/ "ERDF A way of making Europe"), the Project VULNEUREA (Grant PID2021-122290OB-C21 funded by MCIN/ AEI / 10.13039/501100011033 / "ERDF A way of making Europe"), and the project SEGVAUTO-4.0-CM (Grant S2018/EMT-4362 funded by the Community of Madrid). It can be broken down into the following stages: in-depth study of an INSIA UPM accident database, conducting an investigation of the scenario of each collision, and the generation of a predictive collision model by analyzing the pedestrians behavior in potential hit-and-run situations through Virtual Reality tests (green block); on-track tests for the validation of the AEB system in a commercial vehicle, with the aim of analyzing its kinematic and dynamic response, as well as the system's decision logic (dark blue block); the configuration of the joint AEB and AES system by adapting the vehicle model integrated in the CarSim© dynamic simulation software (light blue block); the virtual reconstruction of accidents with the vehicle equipped with the OPREVU-AES and AEB system and without the on-board ADAS system (real accident) in PCCrash® (grey block), estimation of the ISP in the assumptions contemplated in the virtual reconstruction (yellow block), and evaluation of the effectiveness of these systems based on the ISP estimation (orange block).

Preprints (www.preprints.org) | NOT PEER-REVIEWED | Posted: 25 November 2022 doi:10.20944/preprints202211.0476.v1

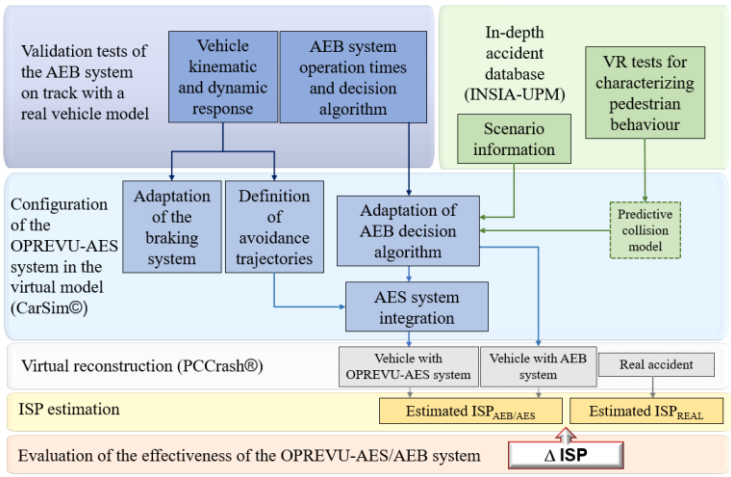

Figure 1. Methodology main scheme of the OPREVU-AES modeling procedure and evaluation of its effectiveness.

3.2. Accident study and virtual reconstruction

To investigate and reconstruct a sample of hit-and-run accidents in Madrid, a multidisciplinary team was set up with the support of local police forces, emergency services and hospitals.

The sampling was based on three main criteria: first, according to the characteristics of the road, the selected accidents must occur in urban areas; the second criterion concerns the type of vehicle, considering only accidents in which the vehicle involved is a passenger car, an SUV (Sport Utility Vehicle) or a light van; the third concerns the configuration of the accident, considering only cases in which the pedestrian is hit by the front of the vehicle. No restrictions were imposed on pedestrian characteristics such as sex, age, height, or weight. Aspects such as information related to the victims, the vehicle, type of impact and severity of injuries, the characteristics of the road and the urban environment, ambient light, weather conditions and traffic density were considered for the design of the test scenarios.

Accident scene investigation and data collection has been the first step in the process. The investigation team, in collaboration with law enforcement, went to the scene to gather all available information about the scenario, road geometry, visibility, visual evidence such as tire marks, as well as vehicle damage. Injury information was acquired from emergency services and hospital data and used in the analysis phase to determine the mechanisms of injury.

Thereupon, a database of 100 accidents involving vulnerable users in the city of Madrid (Spain) was studied (INSIA-UPM database). In order to carry out the reconstruction phase, only those accidents where there was a frontal impact, and where there was damage to the windshield, have been considered. Thus, the subsample analyzed included a total of 40 pedestrian crashes.

Once the investigation and data collection phases are completed, the available information is analyzed, reviewed, and prepared for use in the reconstruction using PCCrash® software. The corresponding vehicle is then selected in each case and loaded from the vehicle database available in the software; its characteristics are configured according to the actual vehicle. For this purpose, the frontal geometry of the real vehicles is precisely measured. Based on anthropometric studies [20-21], multibody pedestrian models are defined, representative of the current Spanish population for both men and women, and for a wide range of ages.

Finally, virtual reconstructions of the accidents are performed using PCCrash® reconstruction software. The initial conditions have a strong influence on the reconstruction kinematics [22]. Numerous parameters, such as the approach speed (S_a), collision speed (S_c), the trajectory, position, pedestrian movement, maneuvers, and driver sequences are

Preprints (www.preprints.org) | NOT PEER-REVIEWED | Posted: 25 November 2022 doi:10.20944/preprints202211.0476.v1

modified and tested in different combinations in an iterative process leading to a reliable reconstruction (Figure 2), matching both impact points with visual evidence, such as dents or marks, and with injury locations and mechanisms, such as final vehicle and pedestrian positions.

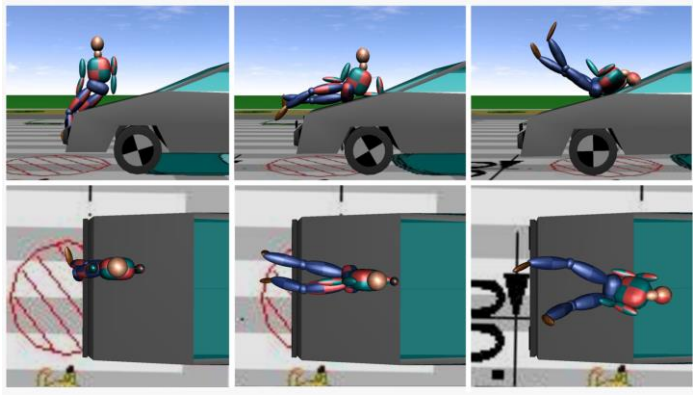

Figure 2. Kinematic sequences of the virtual reconstruction of a vehicle-to-pedestrian collision using PCCrash®

Some upfront hypotheses are established so that all reconstructions are executed from a common approach:

1. The driver's reaction time is 1s in all cases.
2. The delay for a conventional braking system is 0.25 s.
3. The Possible Point of Perception (PPP) of the driver is the moment when the pedestrian steps on the pavement and no obstacle covers the driver's field of vision.
4. Three levels of intensity are set for braking force before the collision: no braking, when evidence shows that the driver did not have time to react or was completely unaware of the presence of pedestrians in the vehicle's lane; medium intensity braking, the default for most crashes; and full braking when evidence, such as tire marks, indicates this.

The distribution of approach speed (S_a) and collision speed (S_c) in the sample accidents is shown in (Figure 3). The probability of a pedestrian being killed in an accident increases with the speed at which the impact with the vehicle occurs. Thus, while in a hit-and-run accident at 30 km/h the probability of suffering fatal injuries is 10%, this probability rises to 80% at 50 km/h and is close to 100% from 60 km/h, according to a review of WHO and OECD/ECMT research [23]. In the sample of collisions analyzed in this document, the collision speed exceeds 30 km/h in 62.8% of the cases, and 50 km/h in 11.6% of the cases.

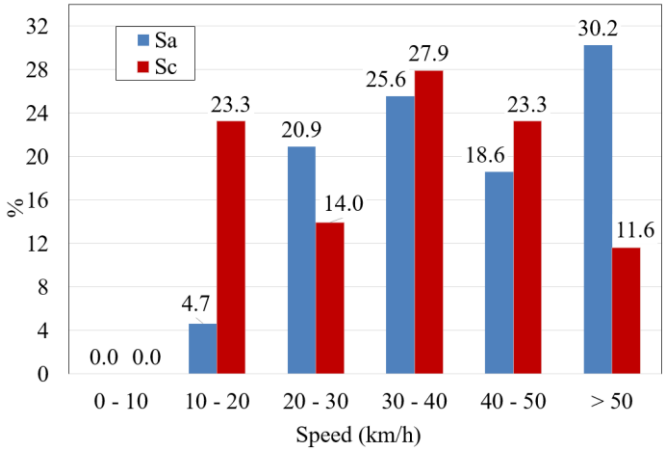

Figure 3. Distribution of approach speed (S_a) and collision speed (S_c) in the sample accidents

Preprints (www.preprints.org) | NOT PEER-REVIEWED | Posted: 25 November 2022 doi:10.20944/preprints202211.0476.v1

3.3. Estimation of Injury Severity Probability (ISP)

Head injuries are usually the most serious injuries suffered by pedestrians when impacted by a vehicle. This severity depends on a large number of parameters such as: collision speed S_c, the point of impact of the head or the rigidity of the struck component on the front of the vehicle.

The intensity of head impact is usually assessed using the Head Injury Criterion (HIC) [24]. The HIC can be correlated with the risk of severe injury, which gives a very clear idea of the severity of the head impact. The methodology used in this investigation to estimate the severity of the head injury is described in (Figure 4.).

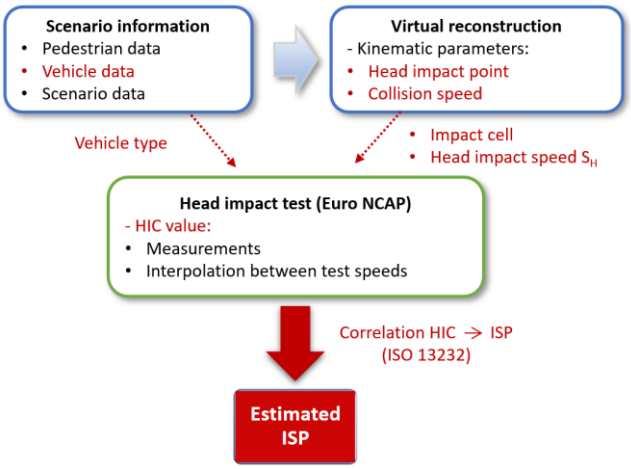

Figure 4. Methodology for estimating the ISP

First, the position of the head impact point is obtained from the virtual reconstruction and is represented by a row and a column corresponding to the WAD (Wrap Around Distance) and the distance across the front DA (Distance across), respectively, according to the front-end division specified by Euro NCAP [25] for pedestrian tests (Figure 5). In the same way, the head impact velocity (S_H) is also obtained from the reconstruction.

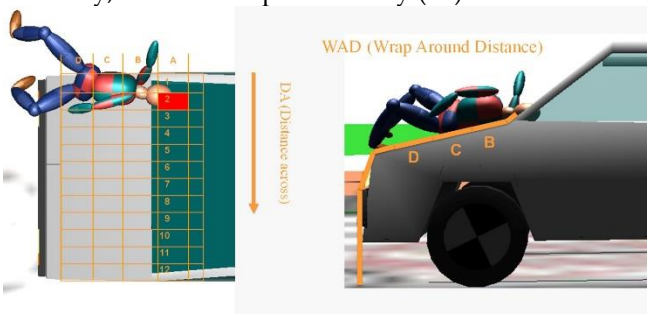

Figure 5. Estimation of the head-on-vehicle front-end impact cell from the reconstruction using PCCrash®

Data from several laboratory tests performed at Applus+ IDIADA are then used to estimate the corresponding HIC, carried out within the framework of the FIT - 370100 - 2007 - 51 project [18]. These are tests conducted for the Euro NCAP pedestrian score using the head impactor for different vehicles, at different speeds, impacting the front of the vehicle. The hard components under the hood, such as the battery and the engine, are considered in correlation with the characteristics of each make and model.

The head impact velocity obtained from the reconstructions is correlated with the closest available velocity from the tests and, if necessary, the HIC value is adjusted by interpolation. Finally, to estimate the severity of the head injury, the estimated HIC value allows to determine the probability of suffering a severe head injury (AIS3+, Abbreviated Injury Scale) ($ISP_{HIC,H,3}$) based on the correlation specified in (Figure 6) [19,26].

Preprints (www.preprints.org) | NOT PEER-REVIEWED | Posted: 25 November 2022 doi:10.20944/preprints202211.0476.v1

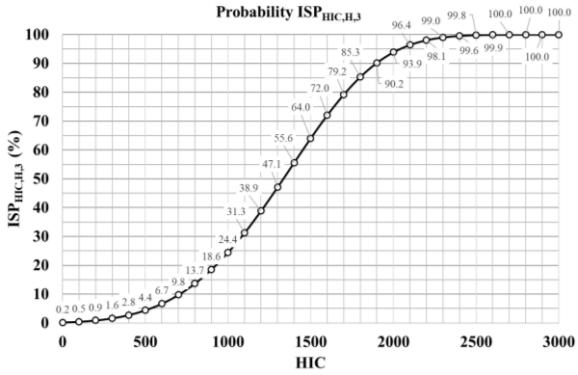

Figure 6. Correlation between the HIC value and the probability of suffering a head injury of AIS3+ severity

The AIS scale was originally developed for use by accident investigators to standardize data on injury frequency and severity. The AIS dictionary is divided into nine sections, corresponding to the different parts of the human body: head (brain and skull); face; neck; thorax; abdomen and pelvis; spine; upper extremities; and lower extremities. Within each section, injuries are assigned a severity code, according to (Table 1).

Table 1. Description of injury severity based on AIS code

AIS Code	Description
1	Minor
2	Moderate
3	Serious
4	Severe
5	Critical
6	Maximum

The distribution of the probability of head injury severity (ISP) in the sample accidents is shown in (Figure 7).

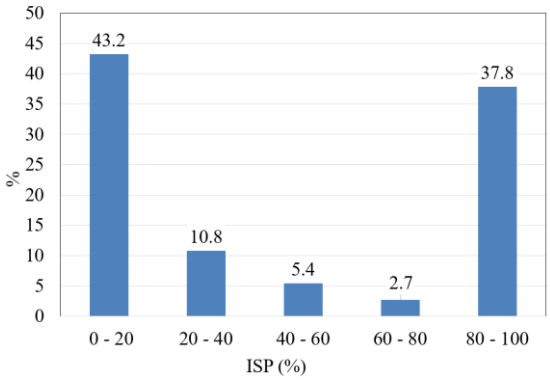

Figure 7. Distribution of the probability of head injury severity (ISP) in the sample accidents

The evolution of the ISP value as a function of the hit-and-run speed in these accidents is also shown (Figure 8). The speed of collision is one of the main variables influencing the ISP value, although it is not the only one. The location of the head impact cell on the front of the vehicle is also of great relevance. Thus:

- In 50% of the cases with very low ISP values (0 - 20), S_c is equal to or higher than 20 km/h, due to head impacts on cells with energy absorption capacity (box in green color in Figure 8).

Preprints (www.preprints.org) | NOT PEER-REVIEWED | Posted: 25 November 2022 doi:10.20944/preprints202211.0476.v1

- In 43% of the collisions with very high ISP values (80 - 100), S_c is equal to or lower than 40 km/h, due to head impacts on cells with high stiffness (red box in Figure 8).

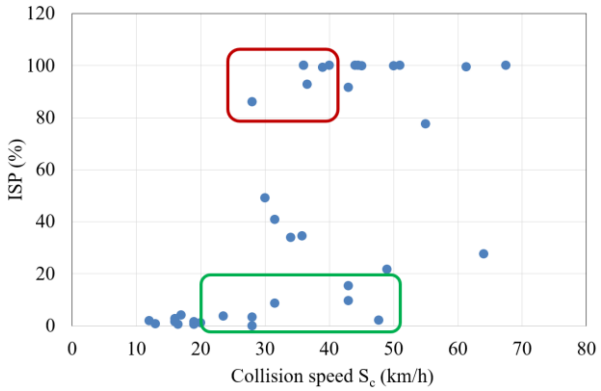

Figure 8. Evolution of the ISP as a function of collision speed S_c in the sample accidents.

3.4. Pedestrian behavior modeling

For the characterization of pedestrian behavior and the generation of a model adaptable to the decision algorithm of the AEB system, the most significant type of collision in the INSIA-UPM database (collision at a crosswalk regulated by traffic lights, with impact at more than 40 km/h in most cases) have been considered. The urban scenarios identified with these hit-and-run characteristics and designed for the experimental session are: Avenida de los Toreros, Avenida de Machupichu and Calle Hermanos García Noblejas.

The tests are performed using an HP GZ V2 Backpack computer, HTC Vive VR glasses, and four base stations to provide the test space with 10x3.6 m dimensions. The tests have been conducted with a sample of subjects with similar sociodemographic conditions (age: 20-30 years; gender: 28% female, 72% male).

From the analysis of the data recorded during the VR tests, it was obtained that: 25.6% of the users accelerated to cross the crosswalk completely to the median; 32.6% stopped and returned to the sidewalk, and 41.8% did not react.

To define the percentage of time that the pedestrian remains looking at the vehicle approach zone, a minimum angle is defined below which the user is considered to be looking at the zone where the vehicle could appear and enter the crosswalk. This angle is defined as "Minimum Angle of Attention, MAA", and takes into account the maximum distance the pedestrian must travel to a point of the crossing where the collision is possible and the minimum distance the piloted vehicle would need to brake completely from cruising speed. The MAA calculations and the geometric definition in the zenithal planes of the streets are shown in detail in the previous paper [27]. For Machupichu, the MAA is αmin=36.9° and for Hermanos García Noblejas, α_{min}=43.3°.

During the data processing phase [27], and after applying an approximation of the minimum redundancy maximum relevance (mRMR) technique for feature selection, four relevant variables were identified in pedestrian behavior and related to the output variable (Avoidance: "0", Collision: "1"): Reaction type (accelerate, stop and step backwards, no reaction), Reaction zone (before hit lane, within hit lane, no speed change), the Percentage of Attention Time (PAT), and the average error (%) made in the distance estimation test in the experimental session in VR. Due to the difficulty of computing this last variable for a system that requires a fast data processing speed, and that would demand access to individual pedestrian information through V2P (Vehicle-to-Pedestrian) technology, the mean error in distance calculation is discarded, and the following variable is chosen as it guarantees the lowest correlation with the rest of the explanatory variables and the highest correlation with the response variables: Street type (reduced visibility, visibility).

Likewise, among the supervised learning classification methods, the formulation of a "White box" type classification method (closer to human logical reasoning, without the mathematical complexity and spatial representation of the so-called "Black box" models)

Preprints (www.preprints.org) | NOT PEER-REVIEWED | Posted: 25 November 2022 doi:10.20944/preprints202211.0476.v1

is proposed. Also, since models whose computational expense is the lowest possible to speed up the processing time in the optimized AEB system are preferred, an individual decision tree model is chosen (Figure 9), whose final accuracy is equal (81%) to that of a Random Forest model (the accuracy has been calculated through a k cross-validation with 5 iterations, and 80/20 distribution in the training/test sample), with the difference that the latter would require a larger number of trees (24 to stabilize the Out-of-the bag, OOB, error rate) and longer execution times.

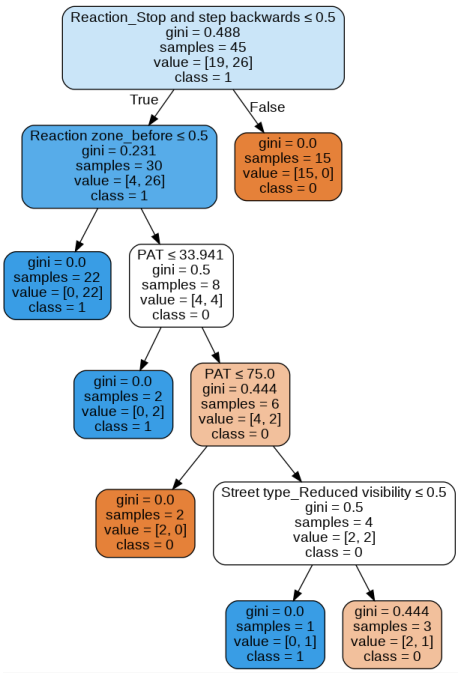

Figure 9. Collision predictive model based on an individual decision tree structure

For those cases where the pedestrian stops and moves backwards, the accident is avoided. In case of accelerating or not reacting, any situation that involves not performing such action before reaching the hit lane will entail an accident. For cases where the pedestrian accelerates early before the lane in which the vehicle is traveling, a PAT value below 33.9% since the vehicle starts the simulation implies an accident; if the PAT value is between 33.9% and 75%, the collision is avoided. For cases where the percentage of PAT exceeds 75%, the crash is only avoided in urban scenarios where there is no visibility.

3.5. Design of OPREVU-AES system and CarSim© integration

3.5.1. Analysis of the commercial AEB system

Track tests have been performed to validate the AEB system in a commercial vehicle (Hyundai Ioniq 1.6 GDI HEV Style DCT), taking as a reference the Euro NCAP CPNA-50 and CPNA-25 (Car-to-Pedestrian Nearside Adult) validation tests [28]. The objective of these tests is to analyze the kinematic and dynamic response of the car during the autonomous braking process, as well as the response times for the Forward Collision Warning (FCW) and for the activation of the automatic braking (Time to Collision-TTC-threshold).

For both configurations, test speeds covered a range between 20 km/h and 60 km/h, with 5 km/h intervals between tests. Additionally, a static dummy was used with the proportions and biometric requirements specified by the Euro NCAP protocol. Vehicle positioning in UTM map coordinates, velocities, accelerations, and moments in the three directions are obtained through a dual antenna recording system incorporated in the vehicle. Data acquisition from the GNSS system is performed at a frequency of 100 Hz.

The data obtained through a dual antenna recording system incorporated in the vehicle are exported and analyzed, yielding the following relevant data:

- The camera covers a range of ±26º (52º amplitude).

Preprints (www.preprints.org) | NOT PEER-REVIEWED | Posted: 25 November 2022 doi:10.20944/preprints202211.0476.v1

- Pedestrian identification is performed at a maximum distance of 30 m (98 ft).
- The lateral distance between the pedestrian and the vehicle (with respect to the longitudinal axis of the vehicle) must be less than 1 m.
- The FCW warning signal is activated when the TTC drops to 1.8 s.

The instantaneous value of the TTC must be less than a certain threshold value for the initiation of autonomous braking, which is variable with the car kinematics. This threshold value for the onset of automatic deceleration is modeled through a linear regression equation: $TTC_{limit}=1.094+0.017 \cdot S_{t=T(D)}-1.225 \cdot D_{mean}$, where S and D are respectively the speed and deceleration and whose goodness-of-fit is $R^2=0.75$ [3].

3.5.2. Definition of OPREVU-AES evasive trajectories

The vehicle system integrated in CarSim© is adapted to the dimensions of the Hyundai Ioniq vehicle tested on track. The masses (suspended and non-suspended), tires, powertrain and steering system are also modified (the original one is replaced by an electronically controlled one, for the subsequent adaptation of the AES system).

In order to generate avoidance maneuvers that guarantee the stability of the vehicle during the complete passing process, point trajectories are defined in the CarSim© double lane change dataset (*Double Lane Change, Tight w/o ESC*), for each of the speeds between 40 and 70 km/h. This speed range has been chosen because below 40 km/h the automatic braking distances of the original AEB never exceeded 12 m, so it is not necessary to establish evasive maneuvers below this speed. Likewise, the collisions analyzed in the database reveal that the maximum speed reached by the cars involved is below 70 km/h, so this is established as the upper limit of action.

In double lane change tests, stable trajectories are obtained between 40 km/h and 55 km/h, 12 m from the pedestrian/target, while between 56 km/h and 65 km/h, the trajectory is stable starting at 18 m from the user. For speeds between 66 km/h and 70 m/h, the distance between the pedestrian and the vehicle at the start of the trajectory must be at least 24 m.

Figure 10 shows the trajectories corresponding to the speed range between 40 km/h (minimum speed for the AES system to operate) and 50 km/h (maximum speed allowed in urban areas), taking the vehicle's center of mass as a reference point. Lines CW represent the width of the crosswalk, and L the lane lines. The performance of the ESC system allows lateral acceleration to be controlled, and in all cases, the steering wheel turning profile and yaw rate allow the conclusion that the overtaking tests (on both sides) comply with the ECE R13H standard [29] for transverse displacement control.

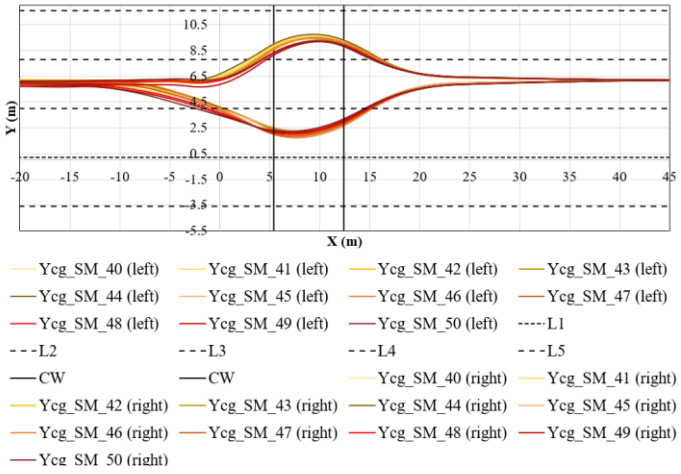

Figure 10. Right and left avoidance trajectories for speeds between 40 km/h and 50 km/h

Likewise, the steering wheel angle has been corrected to ensure that the entry into the overtaking lane is in the center of the lane, with a margin of 0.5 m on each side of the

 doi:10.20944/preprints202211.0476.v1

lane, which guarantees greater safety in the maneuver. Similarly, the detection range (in distance and amplitude) is adapted to the values obtained in the track validation tests.

3.5.3. AEB model setup in CarSim©

The logic algorithm of the AEB system of the virtual model is included in a block system in Simulink, whose input signals are exported from the VS Math model of CarSim©. Originally, in the virtual model the limit values for activation of the FCW warning signal and the TTC for automatic braking are constant. Additionally, there is a preset maximum pressure value, which is constant in all assumptions.

However, it was demonstrated in Section 3.5.1. in the results that the limit TTC value depends on a set of parameters that define the kinematic behavior of the tested vehicle, and subsequently the maximum braking pressure will include a correction factor once the AES system and the optimization of the AEB itself are integrated.

The fusion sensor generates a binary variable, which takes the value of "1" in case of pedestrian detection, and "0" if there is no recognition. In case of pedestrian presence detection, the sensor captures the relative distance and speed between pedestrian and vehicle, bearing angle of the pedestrian with respect to the longitudinal axis, and relative vertical distance between sensor and pedestrian.

The braking system configuration in CarSim© is based on the modification of the first order transfer function that connects the pressure in the master cylinder with the pressure applied directly on the wheel. Consequently, the maximum pressure is adapted considering the deceleration reached in the CarSim© vehicle system for different pressure values during autonomous braking. Considering that the most conservative value of decelerations in the tests with the real vehicle was 0.83g, and that the deceleration curves analyzed in the virtual system tend to stabilize around a value of 0.8g from 70-80 bar, the maximum pressure defined for the activation block of the AEB system is 80 bar.

The value of the time constant (T_d) of the transfer function is responsible for the variation of the constant pressure times during the permanent pressure regime (a higher value of T_d generates a smaller number of steps prior to the continuous pressure regime), as well as for the oscillations prior to the maximum deceleration regime (they are smaller the higher the value of T_d). A higher value of this constant tends to delay in time the point of maximum deceleration, resulting in a more progressive response and a lower maximum deceleration. Comparing the deceleration curves of the real model with those obtained in the virtual model and taking into account that the straight region of the curve, prior to the steady state, is approximately parallel in all cases with an average value of 20 m/s3, it is concluded that the value of the constant T_d is 0.18.

3.5.4. Integration of the predictive collision model and OPREVU-AES setup

Once the primitive virtual model of CarSim© has been adapted, the optimization of the AEB system involves the introduction of the predictive collision model analyzed in Section 3.5.1. The performance limitations of the AEB system analyzed in the original Hyundai model consist mainly of a lateral activation range of 1 m (it covers up to the outermost part of the chassis, 2 m in total), and the non-inclusion of pedestrian behavior and kinematics in the decision algorithm to regulate the braking response, through the predictive collision model.

Subsequently, the set of blocks for the calculation of the following variables are defined within Simulink: reaction type, whose input is the speed of the vulnerable user; the lane of reaction, which requires the relative position of the pedestrian with respect to the vehicle and the relative position of the lanes in which the user is walking in; the PAT, obtained by measuring the rotation of the pedestrian's head; and the detection of lateral obstacles on the roadway (parked vehicles), through the fusion sensor itself. Likewise, the performance margins of the AES and AEB systems are defined, taking into account for the latter the output of the predictive model. For the particular case of the AES system, the information obtained from the rest of the ADAS systems on board in the final model is also considered.

 doi:10.20944/preprints202211.0476.v1

The detection of the frontal vehicle is carried out by the same fusion sensor that allows the identification of pedestrians on the roadway. This sensor measures the distance and bearing angle to the nearest object and to the second nearest object, so in case a pedestrian and a vehicle approaching from the front fall within the detection range of the camera and the LIDAR, the algorithm will process the signal of both, discriminating which one is closer. The identification of each agent on the roadway is done by encoding the type of object. The proximity criterion is based on which object is at the shortest distance on the X-axis, which is a direct function of the distance and bearing angle for each object. The vehicle becomes the closest object when the target volume bounded by the outer face of the chassis exceeds on the X axis the target volume of the pedestrian, represented as a cylindrical body enveloping a dummy with the anthropometric dimensions used in the AEB validation tests. The length of the front vehicle can be calculated as the difference of the distances in X, once the and the type of object changes.

The reaction type is obtained through the speed profile generated by the sensor, and the analysis of the instantaneous acceleration of the sensor. Considering the results of the VR experimental session, the cases whose reaction has been to accelerate correspond to accelerations greater than 1.05 m/s^2, while in cases where the pedestrian brakes and backs up, the deceleration has been greater than 1.05 m/s^2. Pedestrian acceleration is measured through the change in pedestrian speed, so a transport delay block is used to evaluate the signal at two points 0.2 s apart in time. Furthermore, the reaction type is computed by means of a categorical variable, which assigns a numerical value to each motion (*stop and step backwards*=1; *accelerate*=2; *no reaction*=3). Since the minimum distance between the vehicle and the pedestrian to decide is 10 m, in case no change of speed has been detected, the variable reaction type takes the value of 4.

For the calculation of the reaction location, an "If Subsystem" set allows to save the value of the offset lateral in which this change occurred. To evaluate the reaction zone, the information obtained by the 5-points lane detector is used, which processes two signals: *L_Edge_L* for the left lane position, and *L_Edge_R*, for the right lane position, both measured in Y-axis coordinates. If the lateral offset is less than *L_Edge_L* and greater than *L_Edge_R*, the pedestrian reacts within the hit lane, and in case it is less than *L_Edge_R*, it reacts in the upstream lane (note that the Y-axis takes increasing values in the sense of the pedestrian's direction of travel in the crossing).

On the other hand, the calculation of the PAT variable is obtained by capturing the heading angle of the test pedestrian and comparing it with the MAA limit value. It should be noted that, to obtain this value, there is a facial and eye recognition system integrated in the fusion sensor camera itself (including electronic adjustment of the optical zoom). The PAT is computed by means of a first *cumulative sum* block, which acts as the adder of each integration step of the simulation (0.5ms) in which the *heading angle*<MAA. Likewise, another second *cumulative sum* block is used to store the total time of the simulation since the vehicle identifies the pedestrian and the pedestrian moves forward. The quotient between these two times is the PAT. In addition, the identification of vehicles hindering the visibility of the crossing (parked or momentarily stopped) is detected by the camera and LIDAR sensor.

For the design of the AES system, the steering wheel turning, forward coordinate and braking pressure data are exported for each speed and overtaking side, to create a lookup table in the updated decision block system, so that, when activating the avoidance maneuver, the information of these variables is taken. Finally, a blind spot sensor is added, with rear traffic recognition up to 5 m behind the rear of the vehicle. Depending on which flank the rear vehicle is approaching from, this sensor processes the *Alert_R* signals if it is from the right side and *Alert_L* if it is from the left side, generating a raw signal and the corresponding square filtered signal.

The direction of avoidance when the AES is activated is determined by the pedestrian reaction type and the pedestrian's direction of movement when entering the crosswalk. If the pedestrian reacts by accelerating or not reacting, the avoidance is performed with the Type I maneuver, while, in case of stopping and stepping backwards, the overtaking is

Preprints (www.preprints.org) | NOT PEER-REVIEWED | Posted: 25 November 2022 doi:10.20944/preprints202211.0476.v1

performed by turning the steering wheel according to the Type II maneuver. Type I overtaking occurs when the vehicle merges into the lane opposite the one in which the pedestrian is moving towards (if the pedestrian is moving from right to left from the driver's perspective, the initial turn of the steering wheel would be to the right; while if the pedestrian is moving from left to right, the initial turn would be to the left). By the same token, Type II overtaking occurs when the vehicle moves into the same lane as the pedestrian, making the opposite turns of the steering wheel as described for Type I. On the other hand, the value obtained by the collision prediction algorithm takes into account the above values, and its coding has been performed following the decision tree logic discussed in Section 3.4.

The final block with the function integrating the AEB and AES selection yields 3 possible for categorical values for the pressure (pressure:1 for left side avoidance; pressure:2 for right side avoidance; pressure:0 for AEB braking response), and for the steering wheel angle (*SWangle*:1 for left side avoidance; *SWangle*:2 for right side avoidance; *SWangle*:0 for AEB braking response). Each value of the variables pressure and steering wheel angle correspond to the obtained values of pressure and steering wheel angle for each side avoidance and for each corresponding speed, while the null value of both variables implies the individual AEB response. A switch case block allows to output the value resulting from this final block. Likewise, in case of AEB activation and a null prediction by the Machine Learning collision model, there is a gain factor that multiplies the maximum braking pressure value by 0.70, thus regulating the response in the deceleration process.

Figure 11 shows a schematic of the operation of the decision algorithm of the OPREVU-AES system, considering what was described above.

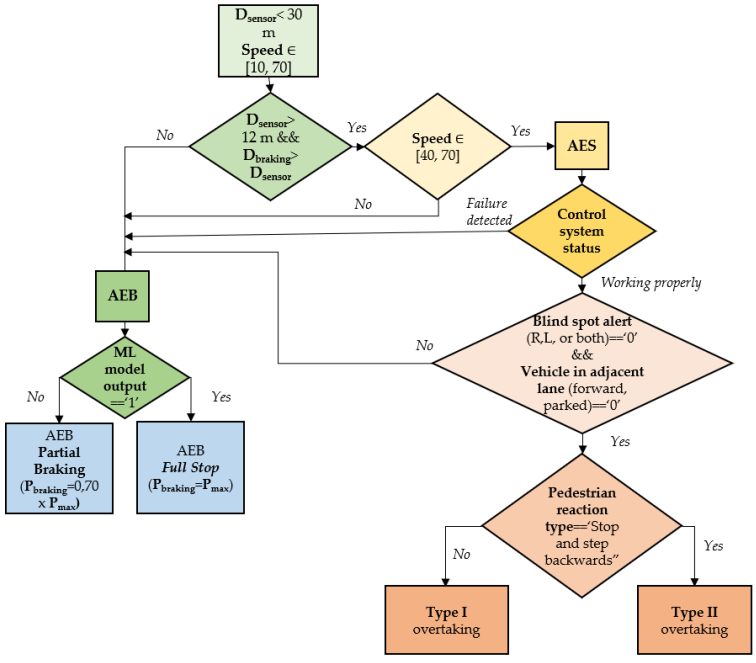

Figure 11. Flowchart of the OPREU-AES system decision making algorithm.

Figure 12 shows a schematic of the detection and actuation range of the OPREVU-AES system, as well as that of the complementary driving assistance systems. The vision range of the fusion sensor is 30 m and total aperture of 52º, and the lateral activation range of the AEB (blue) is 2 m in total. The 5-point lane detection system (purple) allows the position of the lane edges to be obtained. The blind spot detector covers an area of 4m x 5m on each side (orange).

Preprints (www.preprints.org) | NOT PEER-REVIEWED | Posted: 25 November 2022 doi:10.20944/preprints202211.0476.v1

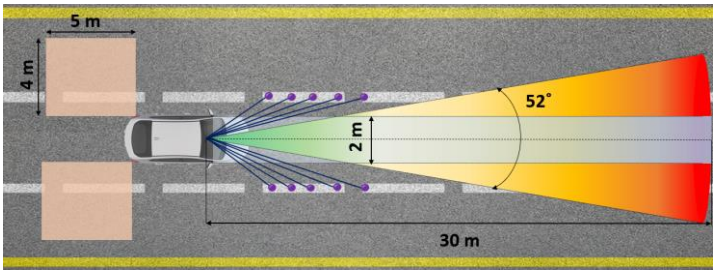

Figure 12. Detection and actuation range of on-vehicle OPREVU-AES system.

4. Results

4.1. Decision-making algorithm of the OPREVU-AES system

If, before reaching the 12 m distance relative to the pedestrian, there is identification of rear traffic or vehicles approaching head-on from either or both sides (detected through the fusion sensor itself), the trajectory is cancelled; while if, once the overtaking has started and the crossing has been passed, there is a vehicle in the original lane, the vehicle deactivates the AES operation and brakes the car with maximum pressure. On the other hand, the decision algorithm of the OPREVU-AES system integrates the information coming from the rest of the car's control systems, so that if a failure is detected in any of them (for example, a flat tire), it automatically overrides the autonomous avoidance process.

In the event that, in a range between 12 m (minimum distance to initiate the overtaking trajectory) and 30 m (maximum sensor range for pedestrian identification), the distance required for braking is greater than the distance relative to the pedestrian in the longitudinal direction, the AES system initiates its operation. Otherwise, the AEB system acts, regulating its braking performance according to the output of the predictive model: in case of potential collision, the maximum pressure of 80 bar is activated; while, in case of predicted avoidance, a braking pressure equal to 70% of the maximum is activated (56 bars), with the objective of guaranteeing a maximum deceleration drop of less than 25% and thus ensuring a safe response (0.64 g).

The choice of this partial pressure is also fostered by the increase in the minimum gap necessary to avoid a rear-end collision between the vehicle equipped with the OPREVU-AES system and another generic vehicle behind it. (Figure 13) shows how would be the evolution of the minimum distance to avoid a possible impact between both vehicles for different values of maximum deceleration during emergency braking. The gain in reaction time for the driver of the following vehicle is also shown. The calculations have been performed considering equal traffic speeds for both vehicles of 30 km/h and 50 km/h, and reaction time of the driver of the rear car of 1 s. The following vehicle brakes with the maximum deceleration (0.83 g) for both cases.

For the case of partial braking of the preceding vehicle, the minimum gap obtained with 70% of the maximum pressure is 1.27 m and 3.52 m for 30 km/h and 50 km/h, respectively. Both values represent 29.7% of the total braking distance at 0.83 g deceleration. On the other hand, the driver of the following vehicle has a gain of 0.15 s for a speed of 30 km/h and 0.25 s for a speed of 50 km/h. For deceleration values higher than 0.64 g, the minimun gap curves and the reaction time gain decrease more progressively, so this deceleration value is optimal to ensure safe braking and less wear on the braking system.

Preprints (www.preprints.org) | NOT PEER-REVIEWED | Posted: 25 November 2022 doi:10.20944/preprints202211.0476.v1

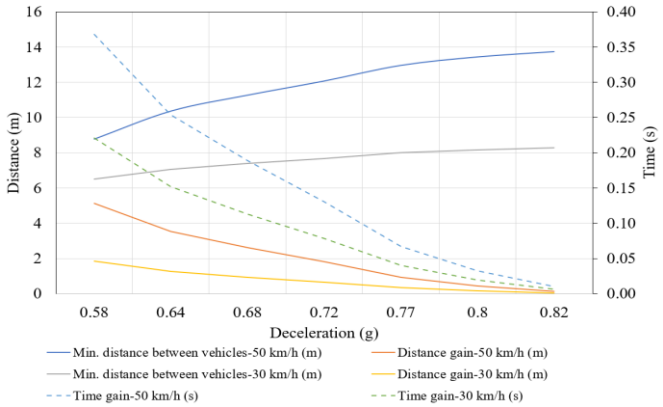

Figure 13. Minimum distance between vehicles, and distance and time gains, for 30 km/h and 50 km/h, after applying a partial emergency braking.

Figure 14 shows an example of the decision making of the combined autonomous braking and avoidance system when faced with a pedestrian accelerating at the crosswalk after seeing the vehicle. In the image on the left (a), the vehicle recognizes rear traffic by blind spot and pedestrian detector and vehicle in front by the fusion sensor. In this case, it overrides the evasion and enables AEB. In the image on the right (b), there are no vehicles in the dodging lane. Therefore, it initiates the passing maneuver.

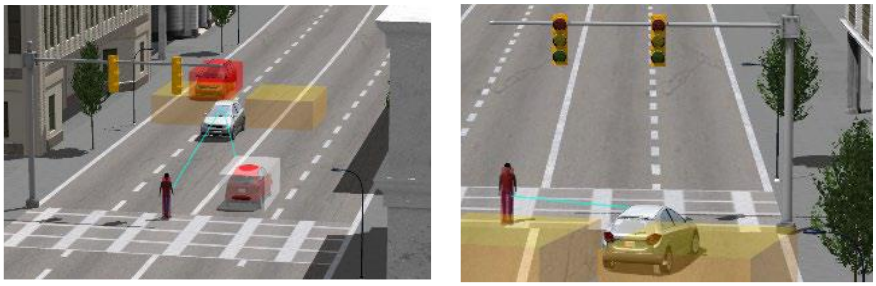

(**a**) (**b**)

Figure 14. Simulation in CarSim© of the OPREVU-AES system for pedestrian accelerating

4.2. Effectiveness of the conventional AEB system and OPREVU-AES in the reconstruction of real accidents

Applying the proposed methodology, each of the pedestrian accidents in the sample has been reconstructed three times:

1. Under real conditions, based on the information collected at the scene of the accident (Figures 3, 7 and 8).
2. Considering the modification of the pre-crash phase through the installation of the commercial AEB system.
3. Simulating the pre-crash phase by installing the OPREVU - AES system.

In each of the cases, the variation of the collision speed and of the head injury severity probability (ISP) after the incorporation of the two systems considered, AEB and OPREVU-AES, has been evaluated. The change in the collision speed due to these systems also implies a modification of the impact cell of the head on the front of the vehicle, both variables influencing the value of the final ISP.

4.2.1. Commercial AEB system

The installation of the autonomous emergency braking function, present in the two systems proposed in this document, makes it possible to avoid 53.8% of the crashes in the sample ((Fig. 15.), green box). In addition to this, the average reduction of the collision speed in these accidents is 62.7%

Preprints (www.preprints.org) | NOT PEER-REVIEWED | Posted: 25 November 2022 doi:10.20944/preprints202211.0476.v1

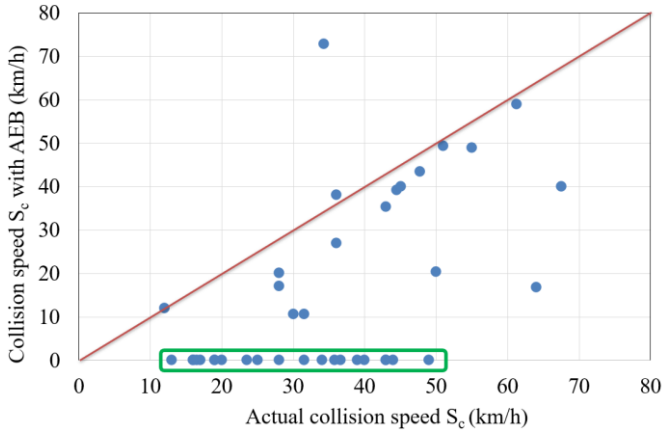

Figure 15. Comparison of the actual versus the collision speed after the installation of the commercial AEB system commercial AEB systems

This avoidance capacity is conditioned by the speed of the vehicle in the moments prior to the collision, and by the speed of the pedestrian (Figure 16) since the pre-impact activation time is related to the instant at which the pedestrian enters the narrow activation zone of the AEB system. Increasing traffic and pedestrian speeds reduce the avoidance possibilities of this device. the chances of avoidance of this device.

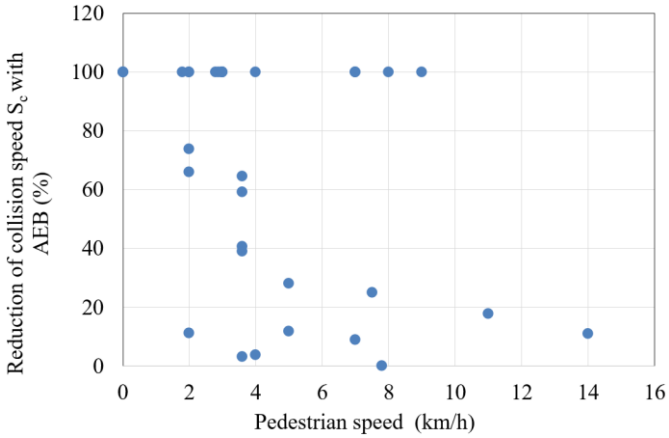

Figure 16. Reduction of the collision speed vs. pedestrian speed after installation of the commercial AEB system

In addition to the above, the ability of the AEB system to reduce the probability of head injury severity (ISP) is shown in the following figures (Figure 17 and Figure 18). The average reduction of the ISP in the sample crashes is 65%; and in 64% of the cases the reduction of the probability of head injury severity exceeds 80%.

Preprints (www.preprints.org) | NOT PEER-REVIEWED | Posted: 25 November 2022 doi:10.20944/preprints202211.0476.v1

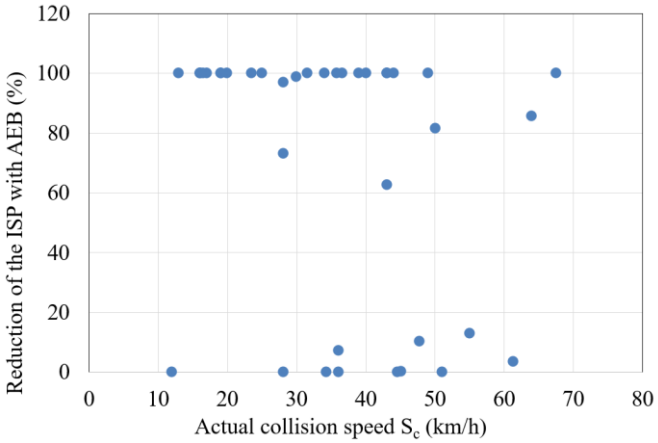

Figure 17. Reduction of the ISP vs. the actual collision speed after installation of the commercial AEB system

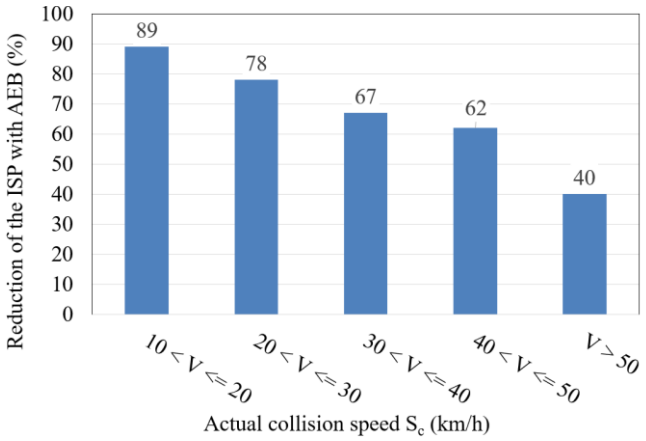

Figure 18. Average reduction of ISP by actual collision speed ranges, after installation of the commercial AEB system

4.2.2. OPREVU-AES system

As described above, the OPREVU-AES system incorporates the autonomous emergency braking function of the commercial AEB system. Therefore, the effectiveness described in the preceding section also applies to the new avoidance system (53.8% of the crashes in the sample could be avoided incorporating the commercial AEB system)..

The OPREVU-AES system requires a minimum distance to the pedestrian to perform the maneuver safely: from 12 m (traffic speed between 40 km/h and 55 km/h) to 24 m (traffic speed between 66 km/h and 70 km/h). Therefore, the possibility of carrying out this evasive maneuver is conditioned by the early detection of the pedestrian, as well as by the constraints of the surroundings of the collision. In addition, the direction of avoidance when the AES function is activated is determined by the pedestrian reaction type and the pedestrian's direction of movement when entering the crosswalk (Figure 11).

46.2% of the accidents in the sample are not avoidable using only the commercial AEB system. And in 5% of the crashes, it is not possible to perform an avoidance maneuver due to infrastructure restrictions (single-lane roads). If the pedestrian does not react (more conservative status of the system) and considering the activation zone of the commercial AEB system, the new OPREVUAES system could avoid 2.5% of the cases (Figure 19). In the rest of the cases (38.7%), the effectiveness of the new avoidance system requires the extension of the activation area in lateral direction above 2 meters. If the activation zone is increased laterally up to 3 meters, this system could avoid 8% of the pedestrian accidents.

Preprints (www.preprints.org) | NOT PEER-REVIEWED | Posted: 25 November 2022 doi:10.20944/preprints202211.0476.v1

If the pedestrian reacts stopping and stepping backwards and considering the activation zone in lateral direction above 3 meters, the OPREVU-AES system could avoid 16% of the cases.

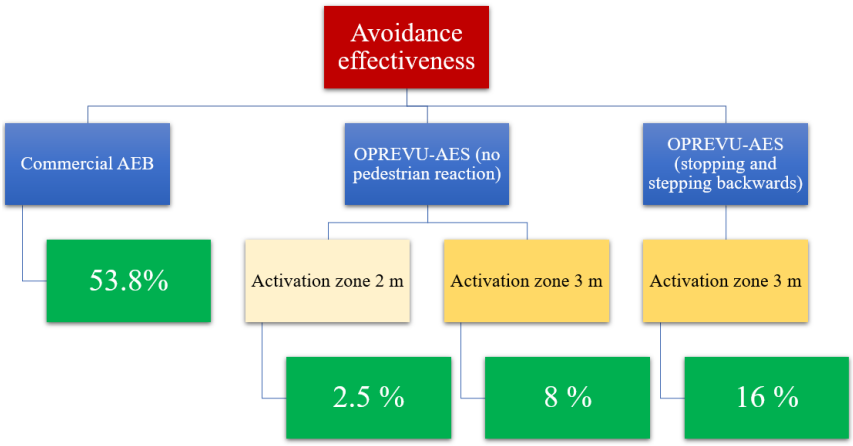

Figure 19. Avoidance effectiveness of the commercial AEB system and OPREVU-AES system

5. Conclusions

Through the proposed methodology, a database of 40 collisions is elaborated, including detailed vehicle, pedestrian (age, weight, height, injury coding, motion kinematics), and scenario information. Reconstructions of these crashes are performed using advanced simulation techniques to accurately estimate multiple parameters of the collision, as well as the pre- and post-impact phases.

The information collected has been used to evaluate the effectiveness of two primary safety systems, a commercial AEB system and the OPREVU-AES autonomous braking and avoidance system. The performance of these systems has been modeled in reconstructions, analyzing their ability to reduce the severity of sample pedestrian collision.

The current OPREVU-AES system enables efficient braking and avoidance maneuvers with automatic steering wheel control, ensuring vehicle stability during the entire overtaking trajectory. Furthermore, the predictive collision model, based on real user behaviors in potential hit-and-run situations in VR environments, allows regulating the braking response when autonomous braking is initiated, making less wear on the braking system plausible.

The set of decision blocks of the AEB and AES systems, in combination with the rest of the driving assistance systems, is capable of processing information every 0.5 ms, making it a low computational load algorithm and capable of executing actions on the vehicle immediately. The merging sensor and the blind spot detector make it possible to evaluate the presence of other agents on the road to ensure that the maneuver is performed safely. On the other hand, the lane line detection system makes it possible to measure the relative positioning of the pedestrian on the roadway and at the same time control the position of the vehicle while executing the overtaking and return maneuver during automatic avoidance.

Performing this type of trajectory implies having sufficient space to execute the maneuver (especially at high traffic speeds), so, within the possible areas of improvement for this technology, it would be necessary to have a camera with a greater range of longitudinal distance. Also, one of the possible limitations of this system is the lack of integration of a multimodal mapping system, capable of jointly processing the information coming from the camera for lane line detection, traffic sign and traffic light recognition; from LIDAR for obstacle detection; and GNSS, to obtain information on the location, speed, and orientation of the car. In addition, future V2P (Vehicle-to-Pedestrian) technology will enable direct or indirect communication (through urban infrastructure) between car and

vulnerable user, so that it will be possible to incorporate pedestrian trajectory prediction into the current collision probability model, achieving greater precision in decision making.

Numerous investigations in recent decades have concluded that the probability of a pedestrian being killed or seriously injured in an accident increases with the speed at which the impact with the vehicle occurs. However, the characteristics of the head-on-vehicle impact cell are also of great relevance. The effectiveness of the autonomous emergency braking function, present in both systems (commercial AEB and OPREVU-AES), is verified by its ability to avoid 54% of the crashes in the sample and by the average ISP reduction of 65%, after its installation on the vehicles involved.

The collision avoidance function of the proposed new OPREVU-AES system presents a great potential for primary safety improvement. However, this function requires a minimum distance to the pedestrian for the safe execution of the maneuver. Increasing the effectiveness of the system requires increasing the activation area in lateral direction above 2 meters. The new automatic evasive function of the OPREVU – AES system could avoid 16% of the cases if the pedestrian reacts stopping and stepping backwards and considering the activation zone in lateral direction above 3 meters.

Author Contributions: Conceptualization, Á.L., F.J.P., F.L., and L.P.; methodology, Á.L., F.J.P., and L.P.; software, Á.L., F.J.P., F.L., and L.P.; validation, Á.L., F.J.P., and L.P.; formal analysis, Á.L.; investigation, Á.L., F.J.P., F.L., and L.P.; resources, F.J.P., F.L., and L.P.; data curation, Á.L.; writing—original draft preparation, Á.L., and F.J.P.; writing—review and editing, Á.L., F.J.P., F.L., and L.P.; visualization, Á.L., F.J.P., F.L., and L.P.; supervision, Á.L. and F.J.P.; project administration, F.J.P.; funding acquisition, F.J.P. All authors have read and agreed to the published version of the manuscript.

Funding This research was funded by the Project OPREVU Grant RTI2018-096617-B-100 funded by MCI/AEI/10.13039/501100011033/ "ERDF A way of making Europe", EU; by the Project VULNEUREA Grant PID2021-122290OB-C21 funded by MCIN/ AEI / 10.13039/501100011033 / "ERDF A way of making Europe", EU; and partially funded by the Community of Madrid (S2018/EMT-4362) SEGVAUTO-4.0-CM.

Informed Consent Statement: Informed consent was obtained from all subjects involved in the study.

Data Availability Statement: Not applicable.

Acknowledgments: This study benefited from the research activities developed by INSIA-UPM and CEDINT-UPM within the OPREVU project, VULNEUREA project and SEGVAUTO-4.0-CM scientific programme. The authors would like to thank Hyundai Motor España S.L.U., as well as experts from the Spanish Traffic Police and the Dirección General de Tráfico (DGT) for their contribution.

Conflicts of Interest: Ángel Losada, Francisco Javier Páez, Francisco Luque and Luca Piovano report financial support and administrative support were provided by the Project OPREVU Grant RTI2018-096617-B-100 funded by MCI/AEI/10.13039/501100011033/ "ERDF A way of making Europe", EU; by the Project VULNEUREA Grant PID2021-122290OB-C21 funded by MCIN/ AEI / 10.13039/501100011033 / "ERDF A way of making Europe", EU; and partially funded by the Community of Madrid (S2018/EMT-4362) SEGVAUTO-4.0-CM

References

1. Vasuki, P.; Veluchamy, S. Pedestrian Detection for Driver Assistance Systems. In Proceedings of the 2016 International Conference on Recent Trends in Information Technology (ICRTIT); IEEE: Chennai, India, April 2016; pp. 1–4.
2. Zhou, Z.; Peng, Y.; Cai, Y. Vision-based Approach for Predicting the Probability of Vehicle–Pedestrian Collisions at Intersections. *IET Intelligent Trans Sys* **2020**, *14*, 1447–1455, doi:10.1049/iet-its.2019.0665.
3. Losada, Á.; Páez, F.J.; Luque, Francisco; Piovano, Luque; Herrero Villamor, J.J.; Santamaría, Asunción Improvement of the AEB Activation Algorithm Based on the Pedestrian Reaction. In Proceedings of the FISITA World Congress 2021 - Technical Programme; FISITA, September 30 2021.

4. Keller, C.G.; Gavrila, D.M. Will the Pedestrian Cross? A Study on Pedestrian Path Prediction. *IEEE Trans. Intell. Transport. Syst.* **2014**, *15*, 494–506, doi:10.1109/TITS.2013.2280766.
5. Chae, H.; Kang, C.M.; Kim, B.; Kim, J.; Chung, C.C.; Choi, J.W. Autonomous Braking System via Deep Reinforcement Learning. **2017**, doi:10.48550/ARXIV.1702.02302.
6. Kilicarslan, M.; Zheng, J.Y. Detecting Walking Pedestrians from Leg Motion in Driving Video. In Proceedings of the 17th International IEEE Conference on Intelligent Transportation Systems (ITSC); IEEE: Qingdao, China, October 2014; pp. 2924–2929.
7. Euro NCAP Euro NCAP 2025 Roadmap, in Pursuit of Vision Zero Available online: https://cdn.euroncap.com/media/30700/euroncap-roadmap-2025-v4.pdf (accessed on 21 October 2022).
8. Isermann, R.; Schorn, M.; Stählin, U. Anticollision System PRORETA with Automatic Braking and Steering. *Vehicle System Dynamics* **2008**, *46*, 683–694, doi:10.1080/00423110802036968.
9. Ackermann, C.; Isermann, R.; Min, S.; Kim, C. Collision Avoidance with Automatic Braking and Swerving. *IFAC Proceedings Volumes* **2014**, *47*, 10694–10699, doi:10.3182/20140824-6-ZA-1003.00353.
10. Ferdinand, J.; Boliang Yi Trajectory Planning for Collision Avoidance in Urban Area. In Proceedings of the 2016 IEEE Intelligent Vehicles Symposium (IV); IEEE: Gotenburg, Sweden, June 2016; pp. 202–207.
11. Fernandez Llorca, D.; Milanes, V.; Parra Alonso, I.; Gavilan, M.; Garcia Daza, I.; Perez, J.; Sotelo, M.Á. Autonomous Pedestrian Collision Avoidance Using a Fuzzy Steering Controller. *IEEE Trans. Intell. Transport. Syst.* **2011**, *12*, 390–401, doi:10.1109/TITS.2010.2091272.
12. Keller, C.G.; Dang, T.; Fritz, H.; Joos, A.; Rabe, C.; Gavrila, D.M. Active Pedestrian Safety by Automatic Braking and Evasive Steering. *IEEE Trans. Intell. Transport. Syst.* **2011**, *12*, 1292–1304, doi:10.1109/TITS.2011.2158424.
13. Kwon, J.-H.; Kim, J.; Kim, S.; Cho, G.-H. Pedestrians Safety Perception and Crossing Behaviors in Narrow Urban Streets: An Experimental Study Using Immersive Virtual Reality Technology. *Accident Analysis & Prevention* **2022**, *174*, 106757, doi:10.1016/j.aap.2022.106757.
14. Azam, M.; Choi, G.; Chung, H.C. An HMD-Based Pedestrian Simulator for Training and Measuring Individuals Perceptual-Motor Behaviour in Road Crossing. *IJHFE* **2020**, *7*, 325, doi:10.1504/IJHFE.2020.112501.
15. Deb, S.; Carruth, D.W.; Sween, R.; Strawderman, L.; Garrison, T.M. Efficacy of Virtual Reality in Pedestrian Safety Research. *Applied Ergonomics* **2017**, *65*, 449–460, doi:10.1016/j.apergo.2017.03.007.
16. Nie, B.; Li, Q.; Gan, S.; Xing, B.; Huang, Y.; Li, S.E. Safety Envelope of Pedestrians upon Motor Vehicle Conflicts Identified via Active Avoidance Behaviour. *Sci Rep* **2021**, *11*, 3996, doi:10.1038/s41598-021-82331-z.
17. Yao, J.; Yang, J.; Otte, D. Investigation of Head Injuries by Reconstructions of Real-World Vehicle-versus-Adult-Pedestrian Accidents. *Safety Science* **2008**, *46*, 1103–1114, doi:10.1016/j.ssci.2007.06.021.
18. INSIA; Applus IDIADA; CENTRO ZARAGOZA; SERNAUTO *Investigación Industrial En La Protección de Peatones a Partir Del Estudio En Profundidad de Accidentes de Tráfico En Madrid, Zaragoza y Barcelona.*; Madrid, España, 2008;
19. ISO *ISO 13232-5:2005. Motorcycles — Test and Analysis Procedures for Research Evaluation of Rider Crash Protective Devices Fitted to Motorcycles — Part 5: Injury Indices and Risk/Benefit Analysis.*; 2005;
20. Benjumea, A.C. Datos Antropométricos de La Población Laboral Española. *Prevención, trabajo y salud: Revista del Instituto Nacional de Seguridad e Higiene en el Trabajo* **2001**, 22–30.
21. Spanish Ministry of Consumer Affairs *Estudio Antropométrico de La Población Femenina En España*; 2008;
22. Untaroiu, C.D.; Crandall, J.R.; Takahashi, Y.; Okamoto, M.; Ito, O.; Fredriksson, R. Analysis of Running Child Pedestrians Impacted by a Vehicle Using Rigid-Body Models and Optimization Techniques. *Safety Science* **2010**, *48*, 259–267, doi:10.1016/j.ssci.2009.09.003.

 doi:10.20944/preprints202211.0476.v1

23. Spanish Traffic Directorate (DGT) 20 Preguntas Sobre La Velocidad (y Todas Las Respuestas). Tráfico y Seguridad Vial Available online: https://revista.dgt.es/Galerias/hemeroteca/revista/TRAFICO-230-S-Verano-15.pdf (accessed on 18 September 2022).
24. SAE International *Human Tolerance to Impact Conditions as Related to Motor Vehicle Design. J885_201102*; 2011;
25. Euro NCAP Pedestrian Testing Protocol. Version 8.4. Available online: https://cdn.euroncap.com/media/32288/euro-ncap-pedestrian-testing-protocol-v84.pdf (accessed on 24 March 2022).
26. Kuehn, M.; Froeming, R.; Schindler, V. Assessment of Vehicle Related Pedestrian Safety.; Washington DC, United States, 2005.
27. Losada, Á.; Páez, F.J.; Luque, F.; Piovano, L. Application of Machine Learning Techniques for Predicting Potential Vehicle-to-Pedestrian Collisions in Virtual Reality Scenarios. *Applied Sciences* **2022**, *12*, 11364, doi:10.3390/app122211364.
28. Euro NCAP TEST PROTOCOL – AEB/LSS VRU Systems. Version 4.1. Available online: https://cdn.euroncap.com/media/67888/euro-ncap-aeb-lss-vru-test-protocol-v41.pdf (accessed on 20 February 2022).
29. Official Journal of the European Union ACTS ADOPTED BY BODIES CREATED BY INTERNATIONAL AGREEMENTS. Regulation No 13-H of the Economic Commission for Europe of the United Nations (UN/ECE) — Uniform Provisions Concerning the Approval of Passenger Cars with Regard to Braking [2015/2364] Available online: https://www.google.com/url?sa=t&rct=j&q=&esrc=s&source=web&cd=&cad=rja&uact=8&ved=2ahUKEwjhyc6p2rf7AhXOhf0HHXifACMQFnoECA0QAQ&url=https%3A%2F%2Feur-lex.europa.eu%2Flegal-content%2FEN%2FTXT%2FPDF%2F%3Furi%3DCELEX%3A42015X1222(01)&usg=AOvVaw2SJnk-MqXkw6wKAyt9sRm8B (accessed on 7 August 2022).